# ASCAT: A Light-Weight, Low-Cost Scatterometer

David G. Long

Electrical and Computer Engineering Department
459 Clyde Building, Brigham Young University, Provo, UT 84602

## ABSTRACT

The Seasat scatterometer (SASS) first demonstrated that winds could be measured from space using spaceborne scatterometers. Such measurements are crucial in understanding air/sea interaction and in studies of global climate. The success of SASS lead to the development of advanced scatterometers such as the ERS-1 AMI scatterometer (current) and the NASA Scatterometer (NSCAT) (planned for launch in 1996 on the Japanese Advanced Earth Observing System [ADEOS]).

Unfortunately, traditional fan-beam scatterometers such as these consume large amounts of power, are heavy and expensive, and are difficult to accommodate on spacecraft. New scatterometer technologies promise lighter and cheaper instruments in the future. In this paper a scatterometer concept known as ASCAT (A Scanning Scatterometer) is presented. ASCAT is a conically-scanning pencil-beam scatterometer system designed for flight on a small satellite. Coupled with an advanced wind retrieval algorithm, the design concept is inherently very flexible and is suited for a variety of tradeoffs in its design and implementation. Some of these tradeoffs are discussed and associated performance estimates are presented.

ASCAT provides a single, very wide (>1000 km) swath with no nadir gap. Using a single, conically-scanning antenna which traces out a helix on the ocean's surface, ASCAT makes two measurements of $\sigma^o$ at different azimuth angles (but at the same incidence angles) at 25-50 km resolution. An advanced wind retrieval algorithm is used to estimate the wind from the measurements. It estimates the entire wind field over the swath simultaneously without the need for the error-prone ambiguity removal algorithms required by traditional wind retrieval techniques. The wind model-based estimation technique is also less sensitive to noise in the $\sigma^o$ measurements, allowing tradeoffs in the instrument design to reduce the instrument power requirements and the antenna size. Compared to a fan-beam-based design, the pencil-beam ASCAT has a higher signal to noise ratio for each $\sigma^o$ measurement, resulting in high measurement accuracy. Since all of the ASCAT $\sigma^o$ measurements are made at a single incidence angle, geophysical model function refinement efforts can be concentrated in a smaller parameter space resulting in smaller modeling error.

## 1. INTRODUCTION

Satellite observation systems are crucial to the monitoring of the motion of the atmosphere and oceans. In particular, oceanic winds play a key role in driving the oceans and in modulating fluxes between the air and sea. Past observational efforts, using conventionally obtained data, have been severely hampered by the lack of accurate wind measurements with high resolution, global coverage, and frequent sampling. The Seasat Scatterometer flown in 1978 first demonstrated the capability of scatterometers to obtain the needed measurements of near-surface vector winds from space.

Although wind scatterometry is an indirect technique, scatterometers are widely recognized as the only all-weather instruments capable of measuring vector winds from space. As a result they play a crucial role in current and future Earth remote sensing systems such as the European ERS-1 and NSCAT.

However, current scatterometer designs are expensive and difficult to accomodate on spacecraft due to their mass, their large antennas which have stringent field of view (FOV) requirements, and their requirement for large amounts of power. These are serious limitations to the continued flights of these crucial instruments. New scatterometer technologies promise lighter and cheaper instrument designs. In particular, a flexible design concept, ASCAT, can provide highly accurate wind measurements at lower cost and with fewer spacecraft resources (i.e., less mass and power) than traditional fan-beam designs. The ASCAT concept permits simple tradeoffs in wind measurement performance and swath versus power requirements and mass.



0-8194-1171-X/93/$6.00

After considering the basis of scatterometry, the ASCAT design concept is described and some of the possible design tradeoffs are discussed. A sample design is then presented along with the estimated wind measurement performance. Finally, a summary conclusion is given.

## 2. PRINCIPLES AND HISTORY OF SCATTEROMETRY

A good review of *Ku*-band wind scatterometry can be found in *Naderi et al.*[3]; however, a brief summary of relevant points will be given here. A wind scatterometer does not directly measure the wind, but measures the radar backscatter of the ocean's surface which is related to the wind via a geophysical model function. To measure the radar backscatter, the instrument transmits a pulse of RF energy and measures the backscattered power. From knowledge of the parameters of the radar equation, the normalized radar cross-section (denoted $\sigma^o$) of the ocean's surface can be computed. The near-surface wind vector is then estimated from the $\sigma^o$ measurements using a geophysical model function. Due to the nature of the geophysical model function (which exhibits a bi-harmonic dependence on the wind direction), multiple co-located measurements of $\sigma^o$ from different azimuth angles are required to determine the wind vector at the ocean's surface. To retrieve the wind, a point-wise wind retrieval approach has been traditionally used in which only the $\sigma^o$ measurements at a single point in the swath are used to retrieve the wind for that point. Because this results in several possible wind directions, a second step, known as "ambiguity removal," is used to determine a unique wind vector

The first spaceborne wind scatterometer was the Seasat Scatterometer (SASS) which flew for 3 months in 1978. The Ku-band SASS used four antennas (two on each side of the spacecraft at angles of 45° and 135° relative to the ground track). It measured $\sigma^o$ at each of two azimuth angles in 600 km wide swaths on each side of the subsatellite track with a spatial resolution of approximately 50 km. This mission conclusively proved that vector winds could be accurately measured from space and led to the developement of future scatteromers such as the NASA Scatterometer (NSCAT) which will fly in 1996 aboard the Japanese Advanced Earth Observing System (ADEOS). In 1991 the European Space Agency launched the Earth Remote Sensing System-1 (ERS-1) which includes a C-band scatterometer. The SASS, NSCAT, and ERS-1 scatterometers all use large fan-beam antennas to measure $\sigma^o$ at different azimuth angles (See Fig. 1).

## 3. SCANNING CONCEPT

Like SASS and NSCAT, ASCAT will obtain measurements of ocean backscatter cross section at Ku-band frequencies near 14 GHz. However, the ASCAT instrument design represents a significant departure from that of past and current spaceborne scatterometers. While SASS, NSCAT, and ERS-1 use multiple fan-beam antennas, ASCAT is based on a conically scanning pencil-beam antenna (Fig. 2). In the sample design described below ASCAT will obtain 50 km resolution measurements of $\sigma^o$ from two azimuth angles over a nominal 1100 km swath width. The scanning is obtained by a fixed off-nadir looking pencil-beam antenna rotating about the spacecraft nadir vector. Figure 2 illustrates the scan pattern relative to the spacecraft nadir. (Since the nadir point propagates on the earth's surface as the satellite orbits, the actual scan patterns on the surface are helixes.) In a circular orbit and with an altitude of 790 km, the ground speed of the nadir point is slightly over 7 km/s. Thus, each beam must complete a full revolution in approximately 8 s in order to achieve the desired mean scan separation of 50 km in the along-track direction.

Each scan images a given point on the surface twice: once when the ocean location is "ahead" of the subsatellite point, and once after the satellite has passed. Thus, two backscatter measurements at 2 different azimuth angles are obtained for each point on the ocean's surface in the swath. By combining both of the backscatter measurements for each ocean location, the surface wind velocity can be estimated.

Compared with the traditional fan-beam scatterometers such as SASS, NSCAT, and ERS-1, the scanning pencil-beam design used for ASCAT has the following advantanges:

1. $\sigma^o$ measurement accuracy: Because radiation is transmitted in a concentrated pencil beam (as opposed to a diffuse fan beam), the high gain of the antenna results in much higher SNR values than for the fan beam at similar incidence angles and the same transmit power. This results in more accurate velocity measurements, especially at low wind speeds where $\sigma^o$ values are small. Alternately, the transmitter's peak power can be lowered to achieve the same measurement accuracy as a fan beam.
2. Continuous swath: The incidence angle for $\sigma^o$ measurements is constant for each scan, independent of cross-track

distance. Thus, the swath is continuous without the nadir gap which occurs in fan-beam based designs. (The nadir gap in the fan-beam based design arises from the lack of azimuthal modulation of the radar backscatter at small incidence angles).

3. Fixed incidence angle: To determine the near-surface wind velocity from scatterometer data, the measured $\sigma^o$ must be related to wind speed and direction via the geophyisical model relating $\sigma^o$ and the wind. Although theoretical work and data analyses have established the basic correlations between $\sigma^o$ and wind velocity, uncertainty in the model function has thus far limited the accuracy of wind velocity estimates based on scatterometer data. A pencil-beam scatterometer design, in which backscatter is measured at only one incidence angle, permits model function refinement efforts to be focused only on the incidence angle used by the instrument.

4. Integral radiometer: The presence of liquid water in the atmosphere can attenuate the scatterometer signal at Ku-band (a problem not enountered at C-band). A separate radiometer has been traditionally used to determine a correction factor for the measured $\sigma^o$; however, a radiometer channel can be incorporated into the ASCAT design. Because the same antenna is used for both the scatterometer and radiometer, the measurements are all coregistered, simplifying ground processing.

5. Processor complexity and data rate: Fan-beam scatterometers such as SASS and NSCAT use complicated on-board Doppler filtering to reduce the data rate and obtain the desired backscatter measurements[3] while range gate scatterometers such as ERS-1 require large data rates and high power transmitters. A pencil-beam design does not require a sophisticated on-board processor, has a small data rate, and can use a low power transmitter. It may be possible to use excess spacecraft capability to collect instrument science and engineering data and to control the instrument operational mode without a separate instrument control system.

The primary disadvantage of a scanning pencil-beam scatterometer is that it requires a rotating antenna assembly. While it is possible to use electronically scanned arrays to avoid using a rotating antenna assembly, the high risk and cost associated with developing a phased-array antenna implementation precludes the use of a phased-array antenna for a low-cost ASCAT design

NSCAT and ERS-1 use 3 azimuth measurements of $\sigma^o$ to determine the wind vector rather than the 2 that SASS used. The extra measurement aids in selecting a unique wind direction during wind retrieval. While the number of azimuth measurements of $\sigma^o$ for ASCAT is comparable to SASS (which suffered from directional ambiguities) an advanced wind retrieval algorithm, which will enable more accurate wind measurements without the direction ambiguity problem associated with point-wise wind retrieval, is proposed to process the data[1,2]. As a result, in spite of its small size, weight and power consumption, the sample ASCAT design described below provides wind measurement performance which exceeds SASS. By adapting the design, ASCAT could be flown on a small satellite which could be launched by Pegasus.

## 4. DESIGN TRADEOFFS

With a pencil-beam design, the performance tradeoff between wind accuracy and instrument design parameters is much more straight-forward than for fan-beam designs. In addition, the performance versus instrument design tradeoff curve tends to be more smooth, allowing gradual degradations/increases in wind performance with design parameter value. While the details of all the design tradeoffs can not be presented in this paper, a brief discussion of two of the key design tradeoff parameters affecting wind performance is presented: transmit power and antenna size (gain) versus wind performance. A comprehensive design tradeoff study was conducted and a sample implementation of the ASCAT design developed. It is described below.

As noted previously, the pencil-beam design inherently has a larger measurement signal-to-noise ratio (SNR) than a fan beam for the same peak antenna gain and transmitter power. Thus, the peak transmitter power can be reduced, with a resultant significant reduction in DC power requirements and cost, while still achieving the same $\sigma^o$ and wind measurement performance. Similarly, the transmit power combined with the antenna gain can be traded against performance. Increasing the size of the parabolic reflector in the rotating antenna will increase its gain permitting a reduction in the transmitter power. Or, the antenna size can be reduced to minimize rotational momentum and simplify spacecraft accomodation requirements by increasing the transmitter power or accepting a reduction in wind measurement performance. We note that the antenna size also affects the illumination spot size (via the beamwidth) and, hence, the resolution.

These tradeoffs can be made by computing the SNR resulting from the design parameters and conducting what-if studies. The SNR (and geometric parameters such as incidence angle) can be related to wind measurement via Monte Carlo simulation. This approach is illustrated below where the antenna size was varied to illustrate the effects on the system performance.

## 5. INSTRUMENT DESCRIPTION

The following is a brief description of the ASCAT instrument conceptual design. This design was developed for an NSCAT-like polar orbit (see Table 1) as an option for a possible NSCAT follow-on mission. *Ku*-band (13.995 GHz) operation was assumed. Effort was made to make as much use of NSCAT designs for RF hardware though this resulted in a more complex design than required. As a result, further refinement of the design parameters is possible.

### 5.1 Overview

In developing the ASCAT design described below, virtually every concession to low-power, minimal weight, and minimal cost has been made consistent with obtaining scatterometer data useful for wind measurement. A conceptual block diagram of the instrument is shown in Fig. 3. .A more detailed system block diagram, emphasizing NSCAT design inheritance, is given in Figure 4. A table summarizing the key instrument parameters is shown in Table 1. A design decision to use separate, off-the-shelf reaction wheels for momentum compensation was made early in the design study to minimize risk and complexity. However, this task could be handled by the spacecraft and/or by counter-rotating wheels.

At the design altitude the antenna beam rotates about the local nadir vector at 7.5 rpm to achieve the desired 50 km resolution. In the baseline design, a spin motor/reaction wheel has been used for mounting on a 3-axis stabilized spacecraft. However, the instrument design could be considerably minimized if the spacecraft provided either a nadir-rotating platform or was spun about the nadir vector.

The baseline antenna consists of an offset feed parabolic disk with a one meter projected aperture. (As previously noted, the antenna aperture can be reduced with some reduction in wind measurement performance.) The antenna reflector points at an off-nadir angle of about 36°. The resulting swath has 50 km resolution and is approximately 1100 km wide with no nadir gap. The antenna feed assembly consists of separate transmit and receive feeds for the scatterometer with additional feeds for the radiometer. The dual scatterometer feed was selected to optimize the reception of the return echo from the ocean's surface due to the long time-of-flight but can be elminated with some sacrifice in calibration accuracy. Separate feeds are used for each of the radiometer channels. The transmitted signal consists of a train of 200-250 $\mu$s 14 GHz interrupted CW transmit pulses with a PRF of ~3.5 kHz.

Very simple low-noise receivers are used for the scatterometer and radiometer channels with a simple on-board power accumulation scheme using fixed range gates and timing to obtain measurements of the return echo and noise-only powers. The echo powers from ten transmit pulses are integrated into one sub-cell power measurement then one noise-only power measurement is made. The power measurements are telemetered to the ground where ground processing will convert these measurements into integrated cell power measurements, thence to $\sigma^o$ and ultimately to winds.

An on-board noise source is used for receiver gain calibration. For system gain calibration, an attenuated transmit pulse is fed into the receiver periodically when the antenna is rotated at 90° relative to the ground track. The signal-to-noise ratio (SNR) at most wind speeds is sufficiently high that the errors in the measurement of the signal power depend principally on the number of transmit pulses accumulated into the radar return power measurement. Hence, the short, frequent pulsing scheme used in ASCAT optimizes the measurement of the signal power and minimizes the measurement error.

The spinning antenna beam and the spacecraft motion along its orbit give rise to a sinusoidal variation in the Doppler center frequency of the return scatterometer echo. This variation is dependent on the known geometry and not on the reflectivity of the ocean surface; hence, the Doppler filter design for the ASCAT instrument can be made quite simple. The filter design is, in fact, less complicated than that used on either SASS or NSCAT. In the baseline design, the received signal is mixed with a variable 3rd IF generated using a single-chip numerically controlled oscillator (NCO). The IF frequency is determined by selecting, as a function of the rotation angle, previously computed digital values from a ROM. Power detection is accomplished by simply squaring and integrating the received signal. Only

a single bandpass filter at audio frequencies is required after the 3rd IF mixing. Power detection occurs at baseband with the squared signal integrated over the range gate sampling interval and sampled with a 12 bit analog to digital converter. The digitized signal is telemetered to the ground for further processing.

### 5.2 Antenna Field of View and Pointing Knowledge

The ASCAT instrument requires a field of view defined by the conical region about the look angle of the antenna. The pointing requirements derive from the timing scheme which requires that the return echo fall between the transmit pulses. The axis of the scan cone may vary from the nadir vector by no more than 0.2° in pitch or roll. The angular difference between the cone axis and the nadir vector must be known to better than 0.2° (if possible). The yaw of the instrument affects only the cell location and the Doppler frequency of the return signal; an error of <1° in the yaw angle is permissible with a knowledge of 0.2° desired.

### 5.2 Telemetry and Data Handling

The estimated instrument science and engineering telemetry data rate (which will be constant for all modes of operation) is less than 5,000 bits per second. This includes science data and instrument health telemetry. Operation is "turn on and forget" with infrequent uploads of small timing tables.

### 5.3 Power Requirements and Mass

The power consumed by the ASCAT instrument depends primarily on the transmitter TWTA peak power. The baseline design described below has an estimated weight of 100 kgs with a power consumption of 100 W (these values include substantial margins and are based on using a 12 W peak output TWTA).

## 6. ASCAT PERFORMANCE

To evaluate the wind measurement performance the design parameters above were used along with the various geometric factors in the radar equation to compute the measurement SNR for various wind speeds and directions at different points in the swath at several orbit positions. A sample dB table is shown in Table 2. Given the measurement SNR and the timing information, the so-called "communication $K_P$" ($K_{Pc}$) was computed. $K_{Pc}$ is the normalized standard deviation of the $\sigma^o$ measurement as a result of radiometric and reciever noise. For the high SNRs encountered by ASCAT, the $K_{Pc}$ is primarily a function of the number of pulses $N_p$ integrated into each power measurement, i.e.,

$$K_{Pc} \approx \frac{1}{\sqrt{N_p}}. \tag{1}$$

For the baseline design $N_p$ varies from 320 to 670 depending on swath location (more pulses are integrated into far-swath cells). For an 8 m/s wind, $K_{Pc}$ is approximately 5% and is roughly constant across the swath. As a result, changes in the system SNR will have only a small effect on the total $K_P$. (This enables further trimming of the antenna size and transmitter power if desirged.)

The total measurement $K_P$ is the root-sum-of-squares of the $K_{Pc}$, the $K_P$ due to geophysical model function error (assumed to be 10%), and the $K_P$ due to uncertainties in the instrument calibration and pointing (assumed to be 10%) . The total $K_P$ is used to generate simulated $\sigma^o$ measurements in simulations described below.

### 6.1 Performance Simulation

Two end-to-end simulation approaches were used, COMPASS and BIGSIM. Both were originally developed for NSCAT performance analysis but have been modified to handle the scanning geometry. The NSCAT COMPASS simulation (described in *Chi and Li*[1]) examines the wind performance at a single measurement swath location by selecting a wind speed and varying the wind direction "around the compass." The simulation can be used for point-wise retrieval only, i.e., ambiguity removal performance evaluation is not possible. The BIGSIM approach (described in *Shaffer et al.*[2]) simulates the flight of the scatterometer over a simulated wind field and is suitable for evaluation of ambiguity removal algorithms and model-based wind retrieval techniques. The NSCAT simulations were modified only as required to treat the scanning geometry.

Based on NSCAT experience with BIGSIM and COMPASS, one must be careful when directly comparing the

results of the two simulations since they have significantly different operating assumptions[5]. While COMPASS examines the performance in a particular cell in great detail as a function of wind speed and direction, the BIGSIM does not concentrate on a single case but looks at spatial effects and is reported differently. As a result, the final RMS error estimates of the two simulations differ slightly. In the simulations, horizontal polarization (which, while having a lower SNR, has improved wind modulation characteristics) and the Wentz model function ("SASS-2") were used.

Note that in traditional point-wise scatterometer wind retrieval only the $\sigma^o$ measurements at a single point are used to estimate the wind at that point. Unfortunately, because the geophysical model function relating the wind and $\sigma^o$ has a bi-harmonic dependence on the wind speed, the point-wise wind direction estimate is not unique and a separate "ambiguity removal" step is required to select a unique wind direction. This problem is ameliorated in model-based wind retrieval.

Figure 5 illustrates the point-wise wind retrieval predicted by the COMPASS simulation. For this particular example, a 20 W TWTA was assumed. To illustrate the tradeoff in antenna gain, Fig. 5a shows the performance for a 1 m antenna while the performance of a 0.75 m antenna is shown in Fig. 5b. The direction errors reported in this figure are based on ideal ambiguity removal. We note that the change in performance due to antenna size is small. The overall performance is quite satisfactory in the outer swath; however, the performance at near-nadir is poor. This is because the two azimuthal $\sigma^o$ measurements are close to 180° appart. The large RMS errors in this region are primarily due to large biases in the wind speed and direction estimates. As a result, we conclude that without improved wind retrieval methods, the near-nadir portion of the swath is not very useful at low wind speeds. This improvement is obtained by using model-based wind retrieval. Thus, for further analysis we must use the BIGSIM simulation approach.

### 6.2 Model-Based Wind Retrieval

One of the limitations of traditional point-wise wind retrieval is the requirement for ambiguity removal, an error-prone and typically ad hoc procedure. Advanced wind retrieval techniques such as model-based wind field estimation (retrieval) can overcome this difficulty. In model-based wind field estimation, a simplified dynamics-based model for the underlying wind field is used. In effect, the $\sigma^o$ measurements are directly assimilated into the model to estimate the wind field. Using the $\sigma^o$ measurements, the model parameters are estimated using maximum-likelihood estimation techniques. The estimated model parameters are then used to compute the wind field. Thus, the estimated wind field is the maximum-likelihood estimate for the field and pointwise ambiguity removal is not required. Model-based wind retrieval uses all the $\sigma^o$ measurements across the swath to estimate the wind field over the entire swath, i.e., it estimates all the wind vectors simultaneously. Based on previous results[1,2,3] the model-based retrieval method 1) can produce more accurate estimates of the wind, 2) has fewer "holes" in the estimated winds, 3) is more robust to $K_P$ changes, and 4) does not require pointwise ambiguity removal. Study results using simulated NSCAT measurements[1,2] and both simulated and actual SASS measurements[3] demonstrate the feasibility and accuracy of this approach.

Based on the results presented below, the use of model-based wind retrieval for processing ASCAT data will allow for 1) relaxed measurement $K_P$ requirements and 2) reduction of the number of antenna beams while maintaining the same wind measurement performance–particularily near-nadir. Note that in this study, the tradeoff capability afforded by the model-based retrieval algorithm was not fully utilized.

In applying the model-based wind retrieval technique, 500 km × 500 km regions with 50% overlap in both the along- and cross-track dimensions were used. The wind field model was second-order for the vorticity and divergence fields and was 8th order for the boundary conditions[1]. This particular region size and layout scheme and these particular model orders were arbitrarily selected. As a result, further study to optimize these parameters is likely to yield improved results.

Model-based wind retrieval can produce multiple fieldwise ambiguities due to the presence of multiple global minima in the objective function. In the most general case, each of the minima are identified and a "fieldwise ambiguity selection" is made. Unlike pointwise ambiguity removal, continuity considerations in the region overlaps can be used to easily resolve the field selection problem. For this paper, the approach[3,6] successfully used with SASS SASS data was used. Based on previous work, this provides results comparable to the full technique[6].

### 6.3 BIGSIM Results

To graphically illustrate the BIGSIM results consider Figs. 6-8. These figures show, respectively, the "true" wind field (Fig. 6), the model-based retrieval result (Fig. 7) and the pointwise ambiguity closest to the true wind (Fig. 8). Note that the subsatellite point propagates from left to right in the center of the wind measurement swath. Several observations can be made from these figures. The model-based result (Fig. 7) very closely resembles the true (Fig. 6) wind field. (There are a few artifacts evident on close inspection; however, these can be minimized by proper weighting of the region overlaps.) In contrast to this result, the closest point-wise field (Fig. 8) exhibits high noise levels in the wind direction, particularly in the nadir region. The potential difficulties in conventional ambiguity removal in the near-nadir region are evident.

These observations are borne out by numerical comparisons of the RMS errors as given in Table 3. Table 3 provides a summary over all the cells across the swath of the mean and RMS error in the wind speed, wind direction, and magnitude vector difference for the model-based estimate and the closest pointwise estimate. Unlike the point-wise retrieval method which varies from unacceptably large at near-nadir to excellent at the far swath, the model-based performance is approximately constant across the swath at an intermediate, but quite acceptable performance. At the far swath the difference in performance of the two retrieval techniques can be attributed to the limitations of the low-order model employed in the model-based retrieval algorithm. Better performance can be obtained (at the expense of increased computation) by using higher-order wind field models. Even so, model-based retrieval provides excellent wind measurement performance over the entire swath. Thus, the use of model-based wind retrieval provides a full-width effective swath.

## 7. CONCLUSION

The high cost and difficulty of accomodating fan-beam scatterometers has lead to the development of alternate scatterometer designs. This paper has considered such a design concept, termed ASCAT, which is based on a conically-scanning pencil-beam antenna coupled with an advanced wind retrieval technique. The resulting design requires significantly less power than the NSCAT design and is lighter and less expensive. An analysis of the performance of ASCAT indicates that it provides high-accuracy wind measurements over a wide swath without a nadir gap. This is due, in part, to the use of an advanced wind retrieval technique known as model-based wind field estimation. While originally developed for a larger spacecraft, the ASCAT design can be scaled down for flight on a small spacecraft such as one launched via Pegasus.

## 7. ACKNOWLEDGMENT

I acknowledge the assistance and encouragement provided by Dr. Michael Frielich of Oregon State University.

## 9. REFERENCES

1. D. G. Long and J. M. Mendel, "Model-Based Estimation of Wind Fields over the Ocean From Scatterometer Measurements Part I: The Wind Field Model," *IEEE Transactions on Geoscience and Remote Sensing*, Vol. 28. No. 2, pp. 349-360, May 1990.

2. D. G. Long and J. M. Mendel, "Model-Based Estimation of Wind Fields over the Ocean From Scatterometer Measurements Part II: Estimation of the Model Parameters," *IEEE Transactions on Geoscience and Remote Sensing*, Vol. 28. No. 2, pp. 361-373, May 1990.

3. D. G. Long, "Model-Based Wind Field Estimation Using SeaSat Scatterometer Measurements," *Proceedings of the International Geoscience and Remote Sensing Symposium*, pp. 545-548, Washington, D.C., May 20-24, 1990.

4. F. Naderi, M. H. Freilich, and D. G. Long, "Spaceborne Radar Measurement of Wind Velocity Over the Ocean–An Overview of the NSCAT Scatterometer System", *Proceedings of the IEEE*, pp. 850-866, Vol. 79, No. 6, June 1991.

| | SASS | ERS-1/2 | NSCAT | NSCAT-2 | ASCAT |
|---|---|---|---|---|---|
| FREQENCY | 14.6 GHz | 5.3 GHz | 13.995 GHz | 13.995 GHz | 13.995 GHz |
| AZIMUTHS | 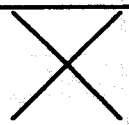 |  | 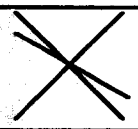 |  | 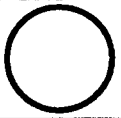 |
| POLAR | V-H, V-H | V ONLY | V, V-H, V | V, V-H, V | H ONLY |
| BEAM RESOLUTION | FIXED DOPPLER | RANGE GATE | VARIABLE DOPPLER | VARIABLE DOPPLER | PENCIL-BEAM |
| SCI. MODES | MANY | SAR, WIND | WIND ONLY | WIND ONLY | WIND ONLY |
| RESOLUTION | 50/100 km | 25/50 km | 25/50 km | 25/25 km | 50 km |
| SWATH | 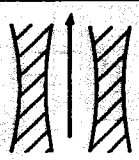 | 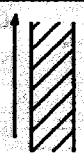 500 | 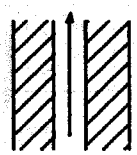 600 600 | 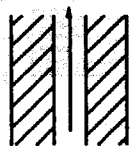 600 600 | 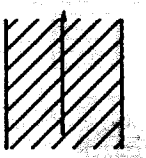 1100 |
| INCIDENCE ANGS | 0° - 70° | 20° - 70° | 17° - 62° | 18° - 65° | 42° |
| DAILY COVERAGE | VARIABLE | <41 % | 78 % | 76 % | 90 % |
| DATES | 6/78 – 10/78 | 91-93 / 94-96 | 2/96 – 2/99 | 1/99 – | 1/99- |

Figure 1. Comparison of past, present, and planned scatterometers.

Table 1. ASCAT Instrument Parameter Summary

| | |
|---|---|
| RF Transmitter | |
| Nominal Frequency | 14 GHz |
| Peak Transmit Power: | 12 W |
| Pulse Length: | 200 ms |
| PRF: | 3 to 4 kHz |
| Duty Cycle: | 65-80 % |
| Receiver | |
| Noise Figure: | 3 dB |
| Dynamic Range: | 50 dB |
| Bandwidth: | 10 MHz |
| Antenna | |
| Reflector Size: | 1 m |
| Pointing Stability: | 0.2° |
| Gain: | 41 dBi |
| Half Power Beamwidth: | 1.2° |
| Rotation rate: | 7.5 rpm |
| Look angle: | 36° |
| Incidence angle: | 42° |
| Orbit | |
| Altitude: | 796 km |
| Inclination angle: | 98.57° |
| Eccentricity: | 0.0011 |
| Argument of perigee: | 90° |
| Interface Requirements | |
| Power required: | 100 W |
| Instrument Telemetry Data rate: | 5 kpbs |
| Mass: | <100 kgs |

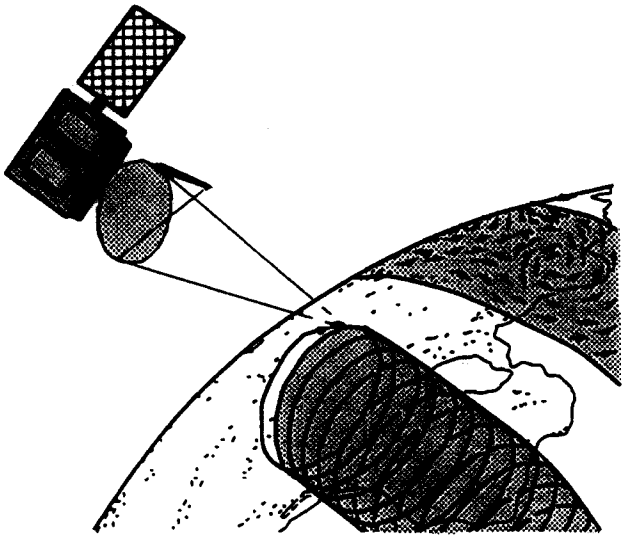

Figure 2. Illustration of the ASCAT design concept showing the scan pattern on the Earth's surface.

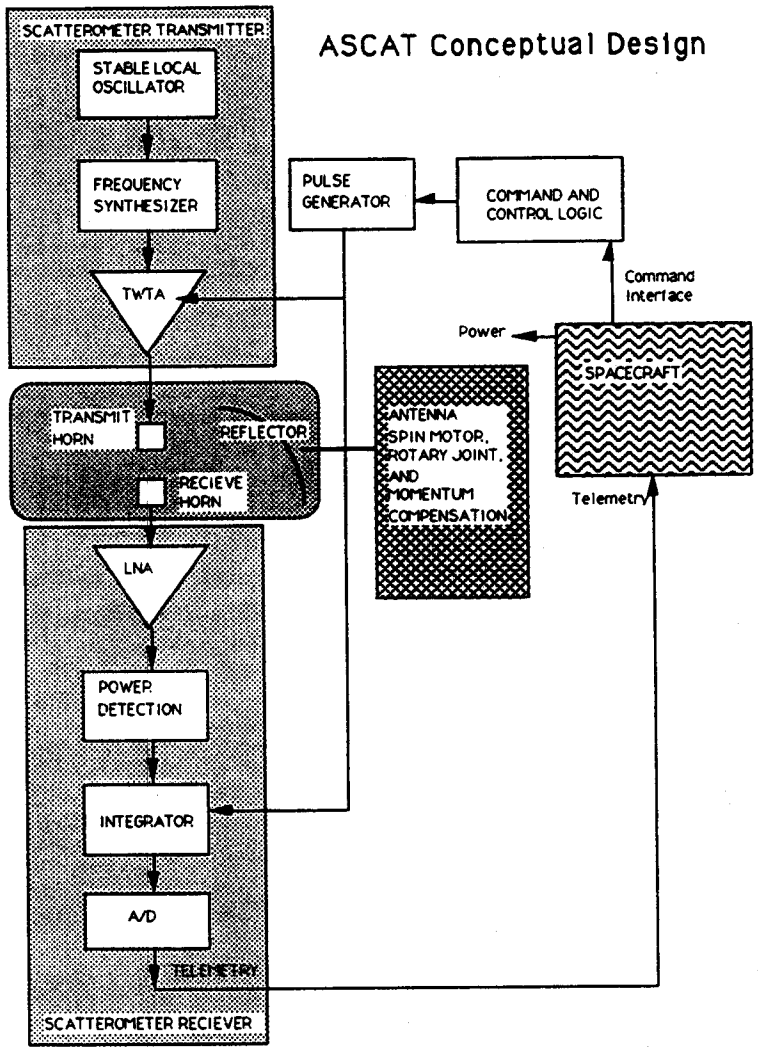


Figure 3. ASCAT conceptual block diagram.

Table 2. Sample SNR/$K_{Pc}$ Table

| | |
|---|---|
| Transmit Power: | 13 dB (20 W) |
| Waveguide System Loss: | -1.2 dB |
| Antenna Gain$^2$: | 82.65 dB (1 m dish) |
| Illumination area: | 86.99 dB (22.4 km)$^2$ |
| Wavelength: | -33.38 dB (2.1421 cm) |
| (4 Pi)$^3$: | -32.98 dB |
| Slant range$^4$: | -240.34 dB |
| Boltzman Const: | -228.60 dB |
| System Temperature: | 28.28 dB |
| Noise Power: | -154.30 dBW |
| SNR/$\sigma^o$ : | 29.05 dB |
| At 8 m/s (average direction) SNR is | -16.9 dB |
| $K_{Pc}$: | 0.05 |
| Signal measurement BW: | 40 kHz |
| Noise-only measurement BW: | 1 MHz |
| Doppler bandwidth: (typical) | 14 kHz |
| PRF: | 3600 pulses/sec |
| Receive range gate: | 49.77 us |
| Pulses integrated: | 320 to 670 |

Table 3. BIGSIM Wind Performance Averaged Over Swath

| | Wind Speed Range (m/s) | | | | |
|---|---|---|---|---|---|
| | 2-4 | 4-8 | 8-12 | 12-20 | 20+ |
| RMS Speed | | | | | |
| Model-based | 0.36 | 0.49 | 0.61 | 0.72 | 1.16 |
| Point-wise* | 0.36 | 0.62 | 0.84 | 1.39 | 0.85 |
| RMS Dir | | | | | |
| Model-based | 11.5 | 6.9 | 6.8 | 5.4 | 4.6 |
| Point-wise* | 25.2 | 19.7 | 16.4 | 17.4 | 9.0 |
| Vector | | | | | |
| Model-based | 0.27 | 0.16 | 0.16 | 0.11 | 0.34 |
| Point-wise* | 0.46 | 0.33 | 0.28 | 0.29 | 0.18 |

* Ambiguity closest to the true wind.

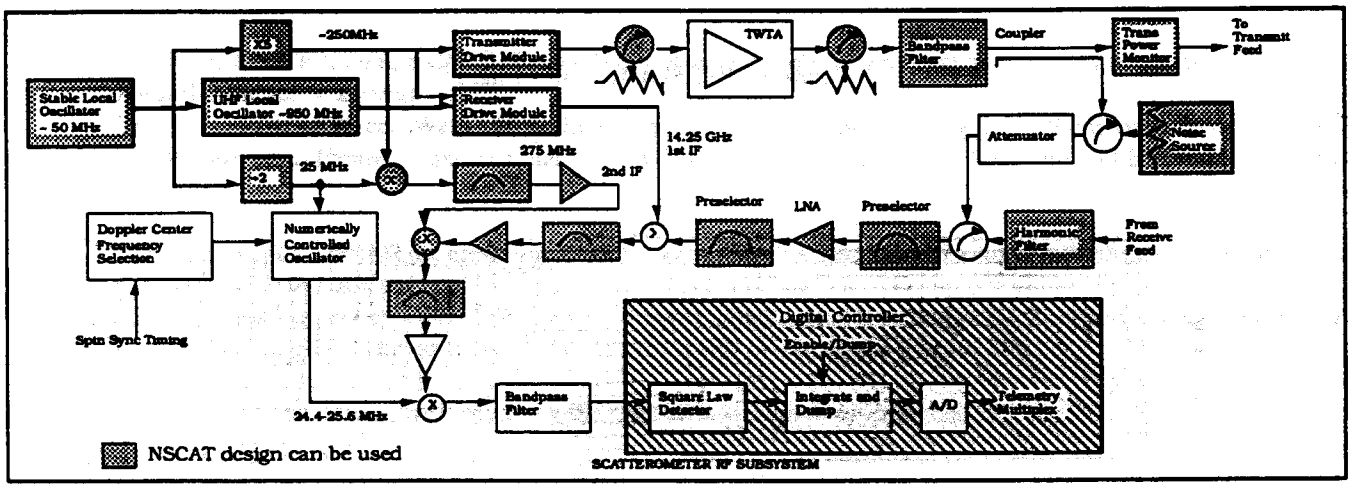


Figure 4. ASCAT system block diagram.

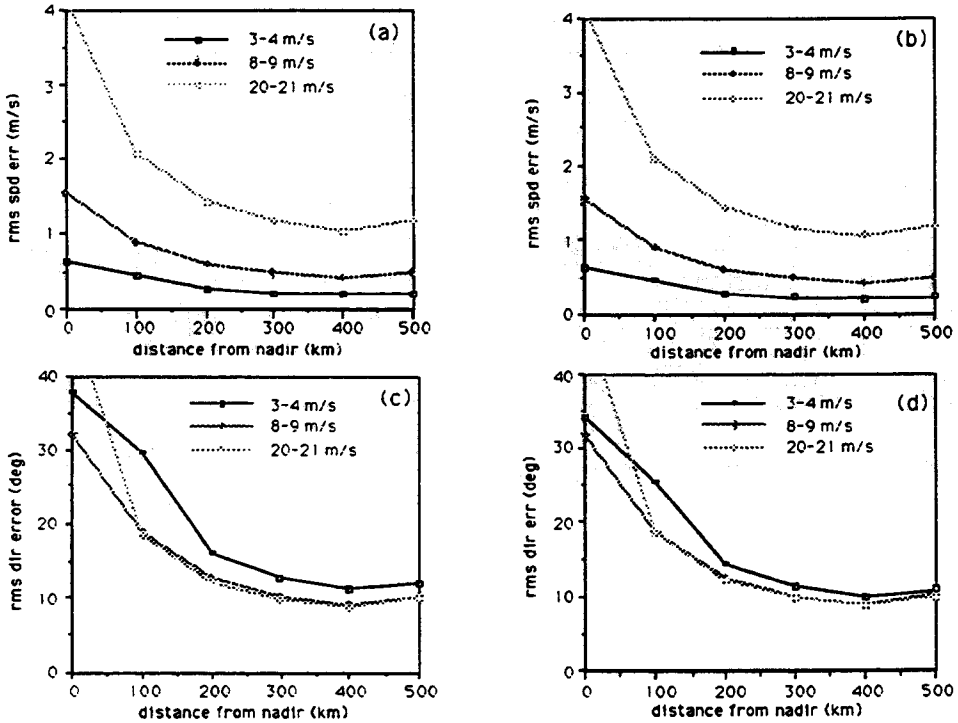


Figure 5. COMPASS simulation results.

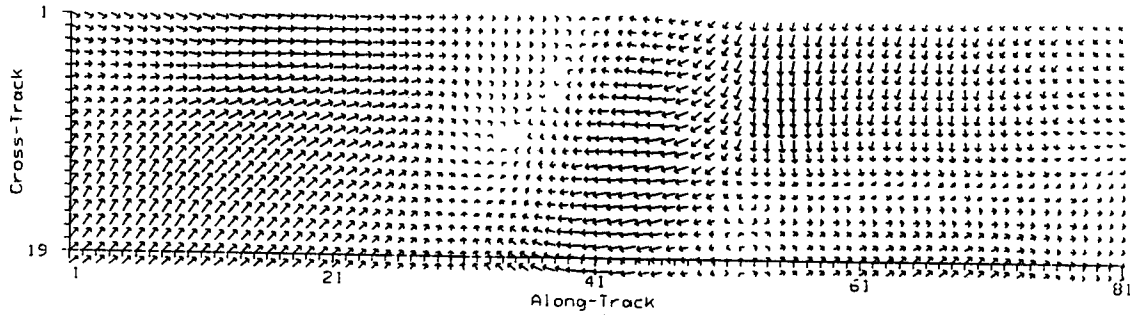


Figure 6. BIGSIM true wind field.

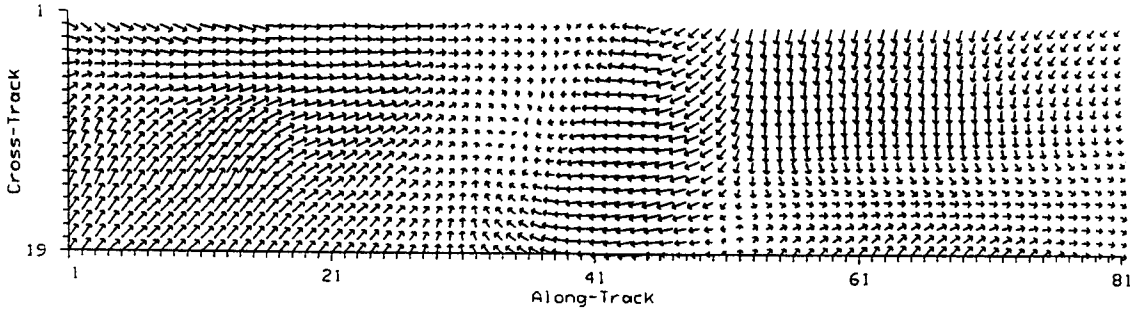


Figure 7. BIGSIM model-based retrieval result.

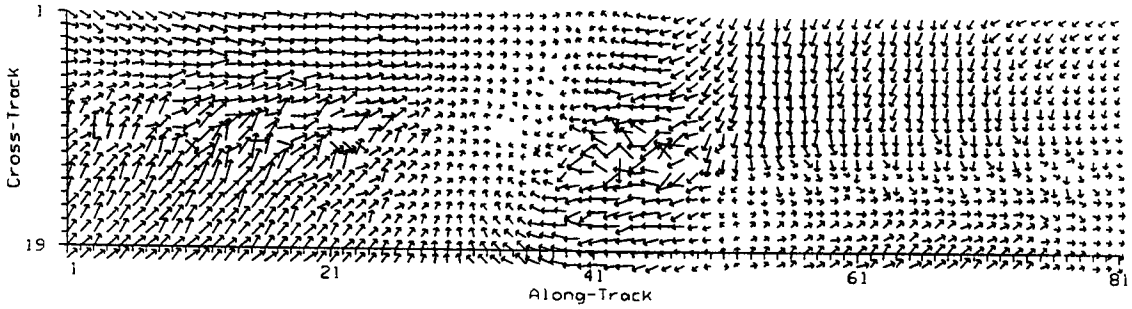


Figure 8. BIGSIM point-wise retrieval with ideal ambiguity removal.